

Research Article

Jawad K. Thajeel, Raghad Adel, Haneen Muhammed Ali, and Ressel R. Shakir*

Effect of the covariance matrix type on the CPT based soil stratification utilizing the Gaussian mixture model

<https://doi.org/10.1515/jmbm-2022-0049>

received April 14, 2022; accepted May 18, 2022

Abstract: The identification and stratification of soils represent an essential step in designing various geotechnical structures. The cone penetration test (CPT) measurements are used widely to classify the soil; however, the soil classification charts such as the Robertson chart undergo uncertainty from different sources that make overlapping of soil types. This article aims to develop a probabilistic approach employing clustering with Gaussian mixture model, which can deal with the uncertainty and classify the soil based on CPT. The spatial parameters were obtained assuming the different types of covariance matrices. The data utilized in this study represent the results of CPT in four locations in Nasiriyah, Iraq. Both spatial and feature patterns were produced and used to classify the soil. This research revealed that the soils deduced from the Robertson chart were clay, silt, and sand. No gravelly sand appeared on the chart. The soil at shallow depth was clay soils, and it changed to be sandy silt at fairly great depth. They were close to the boundary curve between the stiff clay and sand zones and relatively existed at great depth. The probabilistic approach can detect the soil layers fast without experience-based decisions. Moreover, the type of assumed covariance matrix may affect the soil profile.

Keywords: Gaussian mixture model, CPT, soil classification, Nasiriyah soil

1 Introduction

Designing geotechnical structures such as pile foundations based on field tests [1,2], or by numerical methods [3], require preparing the soil classification profile according to the site investigation report because the design formulas or the numerical solutions mainly depend on the type of soil and the thicknesses of layers. One of the widely used field test-based soil classification methods was by Robertson chart, which depends on the cone penetration test (CPT). The CPT has been used increasingly in Iraq despite its high cost [4] compared to other tests since it is fast and gives a continuous reading [5,6]. Two main quantities that can be measured during CPT are cone resistance (q_c) and friction resistance (f_s). The mechanical properties of the soils, such as strength and compressibility, are estimated due to the physical response of the investigated soils to cone advance through the soil, which reveals the idea of CPT-based classification. The relations between soil composition and mechanical properties depend on the complicated environmental condition. Moreover, since the CPT performs no extracted sample, the soil cannot be visually identified. Some of the measurements may give soil classes that are not compatible with the borehole profile. Other uncertainties contain inherent soil variability due to soil's geological process, called aleatory uncertainty [7] or actual variabilities. These include the base resistance and friction, which will be variable and irreducible, mechanical and electrical features of the device, tolerances, operator error, and transformation uncertainties. In addition to that, the classification chart developed by Robertson contains uncertainty that comes from observation scattered, measurement error, and transformation uncertainty. The CPT soil classification charts are generic and may not give accurate results of soil type [8]. Therefore, the interpretation of the CPT results is affected by the uncertainty from different sources. The induced uncertainty cannot be avoided. The CPT-based classification is used to guide classification [9,10]. The CPT classification system is not an alternative to the other

* Corresponding author: Ressel R. Shakir, Department of Civil Engineering, University of Thi-Qar, Thi-Qar, Iraq, e-mail: rrshakir@utq.edu.iq

Jawad K. Thajeel: Department of Civil Engineering, University of Thi-Qar, Thi-Qar, Iraq, e-mail: Jawad.thajeel@utq.edu.iq

Raghad Adel: Department of Civil Engineering, University of Thi-Qar, Thi-Qar, Iraq, e-mail: raghadadel@utq.edu.iq

Haneen Muhammed Ali: Department of Civil Engineering, University of Thi-Qar, Thi-Qar, Iraq, e-mail: haneen1994@utq.edu.iq

methods. They can serve the knowledge integrity, each completing the other. The laboratory systems are limited to the samples while CPT is continuous with depth. We used this test since it is fast and gives a continuous reading and also it is computerized and can give the classification directly.

According to the drawbacks mentioned above, the probabilistic methods may show a critical approach for classifying the soil and providing a confident and reasonable classification, particularly with reliability analysis. Many researchers have investigated the uncertainty in CPT-based soil profiling using statistical models such as statistical criteria [11] and wavelet transform modulus [12]. Since a set of CPT measurements leads to unobserved or hidden soil classes, a Hidden Markov Model was applied to CPT-based classification following the Bayesian approach by Krogstad *et al.* [13]. A Bayesian framework for probabilistic soil stratification has been developed (*e.g.*, [14–17]). A Bayesian clustering approach based on the Hidden Markov Random field with multiple datasets was used by Wang *et al.* [18] to classify the soils. The game theory model was used by Optimizer [19] and sparse modeling by Tsuda and Kagehira [20]. Despite that all these methods tried to probabilistically classify the soil, there is still a need to make an accurate classification without the need to experience-based classification functioning the two components measured by CPT: friction and cone resistance. Besides, an interpretation of distributions to the statistical clusters on the Robertson chart is required for more accurate results. Moreover, the effect of covariance type on soil profile estimating is required.

The main objective of this article is to explore the soil type utilizing the probabilistic framework provided by the Gaussian mixture model (GMM). The GMM is a class of probabilistic approaches that derives the data points from a mixture of a finite Gaussian distribution. The model is applied on four CPTs performed at Nasiriyah city in Iraq. Different assumed clusters are also studied to explore the correlation between cone resistance and friction. The effect of covariance type is studied by using four cases of covariance matrices to represent the soil classification. The current study examines the impact of covariance type on the probabilistic soil classification. It states the application of the suggested approach on CPTs at a site in Nasiriyah, Iraq by developing Matlab codes.

2 GMM

This article utilizes the GMM method since it is efficient and may simulate the data more accurately than other methods such as k -means clusters. GMM is used to cluster the points resulted from mapping base and friction resistance on Robertson chart. It considers the variance equal to the width of the bell-shaped curve of the probability. In two dimensions, variance (covariance) determines the shape of the distribution. It is widely used in data mining, classification, and statistical analysis. The probability density function of the multivariate Gaussian distribution with x input vector is given as follows:

$$f(\ln F_t, \ln Q_t | \pi_k, \mu_k, \Sigma_k) = \sum_{j=1}^k \pi_j \varphi(\ln F_t, \ln Q_t | \mu_k, \Sigma_k), \quad (1)$$

$$f(x | \mu, \Sigma) = \frac{1}{\sqrt{2\pi} |\Sigma|} \exp \left[-\frac{1}{2} (x - \mu)^T \Sigma^{-1} (x - \mu) \right], \quad (2)$$

where u is a 2D mean vector and Σ is the 2×2 covariance matrix which can be defined as follows:

$$\mu = E[x], \quad (3)$$

$$\Sigma = E[(X - \mu)(X - \mu)^T]. \quad (4)$$

The x input vector consists of the friction ratio (F_t) and the normalized cone resistance (Q_t)

$$F_t = \frac{f_s}{q_t - \sigma_v}, \quad (5)$$

$$Q_t = \frac{q_t - \sigma_v}{\sigma'_v}. \quad (6)$$

The parameters of GMM are estimated by using the expectation-maximization algorithm which utilizes the maximum likelihood method.

3 The study area

3.1 Description of the site

The tested site used in this research is situated in Nasiriyah. It is located South-East of Baghdad City, Iraq. The site was



Figure 1: Location of the CPTs [4].

explored to build an oil depot project. The site investigation included four CPTs in addition to boreholes. The model of soil classification was implemented on this site. Figure 1 shows the location of the four CPTs.

From the geological view, the formation of soil encountered in the south of Iraq (e.g., at the city of Nasiriyah), located at the Mesopotamian plain, which contains the alluvial sedimentation deposit from the Tigris and Euphrates rivers. Nasiriyah city is a part of the flood plain region, representing the recent surface formation of Iraq geology, since the site is free from the erosion of old rock surface. The statistical analysis, probability distribution, in addition to spatial correlation of similar sites in Nasiriyah can be found in [21,22]. Further, geotechnical mapping and soil characterization for soils in the same city was reported in [23].

3.2 Measured quantities during CPT

Figure 2 shows the distribution of q_c and also f_s with depth. The index soil behavior (I_c) distribution with depth for every point at interval 0.01 m is also shown. The distribution with depth is also provided in Figure 2c,

Table 1: Zone of soil based on I_c values (Robertson, 2010)

Zone	I_c range	Soil behavior type
1	Not appl.	Sensitive, fine-grained
2	$I_c > 3.6$	Organic soils-peats
3	$2.95 < I_c < 3.6$	Clay, silty clay
4	$2.60 < I_c < 2.95$	Clayey silt to silty clay
5	$2.05 < I_c < 2.60$	Silty sand to sandy silt
6	$1.31 < I_c < 2.60$	Clean sand, silty sand
7	$I_c < 1.31$	Gravelly sand to sand
8	Not appl.	Very stiff sand to clayey sand
9	Not appl.	Very stiff, fine-grained

referring to the soil zone as the region. Figure 2d shows the soil stratification for CPT1.

It is clear that the clay soil is the master layer in the profile, and approximately at 11–12 m; the profile gives clean sand and silty sand (Table 1) and between 14 and 15 m silty sand to sandy silt. For CPT4, clay soil also is the master type of soil.

4 Results and discussions

4.1 Soil classification based on Robertson chart

CPT measured two main components: cone resistance (q_c) and sleeve friction (f_s). The CPT covers a depth of 15 m at an interval of 0.01 m. The measured stresses during CPT were distributed with depth as presented in Figure 2a and b. Figure 3 shows the data pairs ($\ln Q_t$ and $\ln F_t$) along with the Robertson chart. Every point represents an individual representation of the measurements.

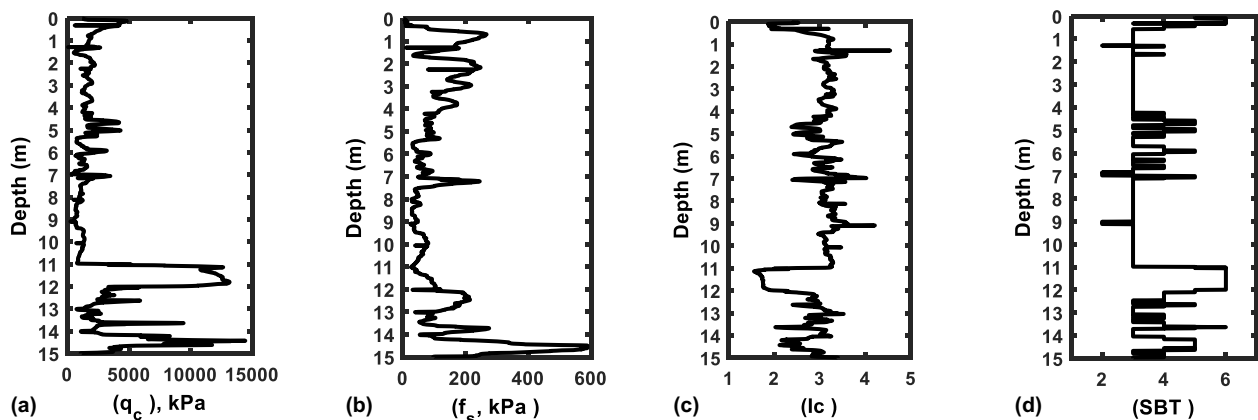


Figure 2: Distribution of basic parameters with depth.

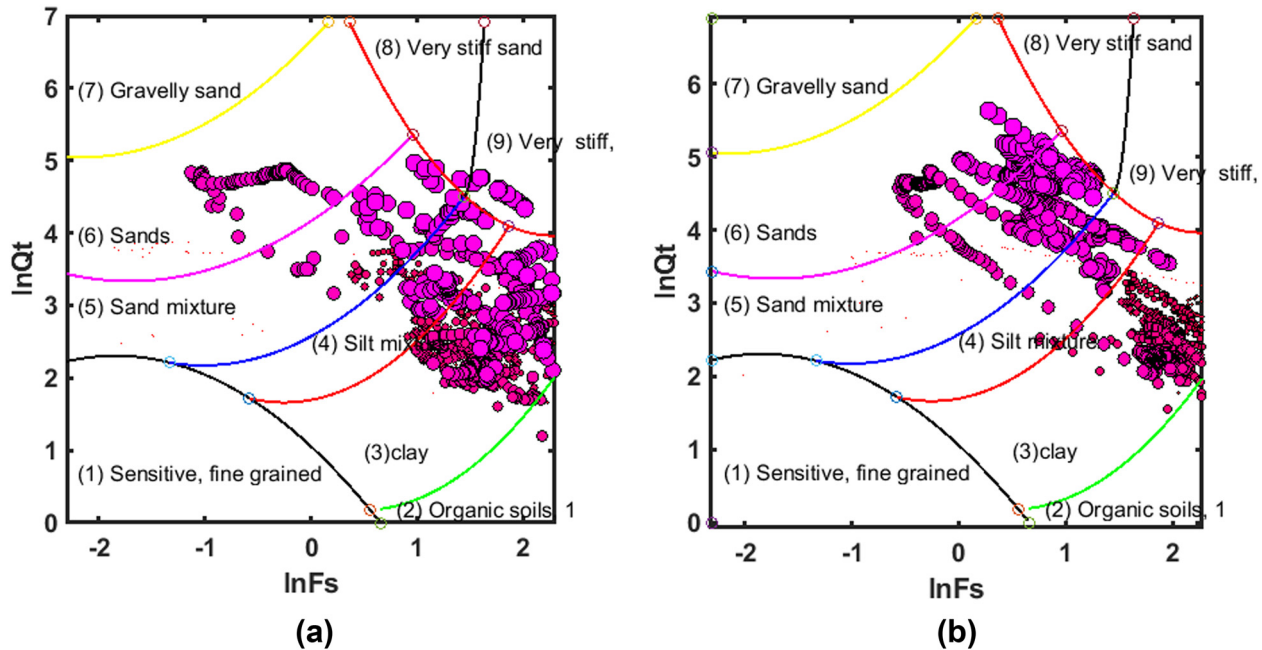


Figure 3: Points of $\ln Q_t$ and $\ln F_s$ in the physical space proposed by Robertson, 2010 and the distribution of soil along the depth. (a) CPT1 and (b) CPT2.

The points are presented so that the size of the circle markers in the plot increases with depth. The data are mainly located in zones 3, 4, 5, and 6 (clay to silty clay, clayey silt to silty clay, silt sand to sandy silt, and clean sand to silty sand) (Table 1). The measured quantities through performing CPTs at this site did not show any gravelly sand soil on the classification chart. Practically, on Robertson chart, the layers' boundaries with depth are unknown and are usually based on the borehole or project-specific test results. However, making the marker size of every point may give an overview of the changing of the layers with depth. The interpretation of Robertson chart shows that the soil type starts to show sand soil with depth. Most of the points tend to be close to the stiff sand and clay curve, especially at relatively great depth. On the other hand, the small circle symbols displayed on the classification chart refer to that the soil at shallow depth is clay soil. Figure 4a and b shows the distribution of measured points on the feature pattern of soil for CPT3 and 4.

4.2 GMM with one cluster applied to CPT

This section presents the results and discussion of grouping the CPT data used for soil classification into clusters utilizing GMM. Since the soil in Nasiriyah is located in the Mesopotamian region which sedimented for thousand years, the data distributed on the Robertson chart

may be assumed for analysis purpose by a single GMM component or a few components. Although the CPT data may be distributed at one cluster on Robertson chart, the result is dramatically affected by the type of covariance matrix. For diagonal covariance (DC), the ellipse represents the data with axes parallel to the main and secondary axes. For the case of DC, the mean value of $(\ln Q_t, \ln F_s)$ pairs was $\mu = [1.5586, 2.9216]$ and the covariance was $\Sigma = [0.7360, 0; 0, 0.5861]$. This case assumes zero correlation because the minor diagonal of the covariance is zero. The ellipse axes parallel to the coordinate axes, which means no rotation (Figure 5a). Using a full covariance matrix for one component GMM reveals the presented ellipse on the Robertson chart as in Figure 5b. The mean value equal to $\mu = [1.5586, 2.9216]$ and $\Sigma = [0.7360, -0.3665; -0.3665, 0.5861]$.

The correlation between $\ln Q_t$ and $\ln F_s$ is negative because of the negative values in the covariance matrix. Here, this correlation means as the $\ln F_s$ increases the $\ln Q_t$ decreases.

For CPT 2, the mean value of the single cluster was $[1.8448, 2.9204]$ and the DC was $[0.9275, 0; 0, 1.4331]$. It was found that the center of the ellipse for all covariance types was in region 3 on the Robertson chart and the soil type was clay, and silty clay soil; however, it is obvious that the center of the data cluster is located near the boundary curve between regions 2 and 3. For the case of full covariance, the mean value of the single component of GMM is $[1.8448, 2.9204]$ and the full covariance is

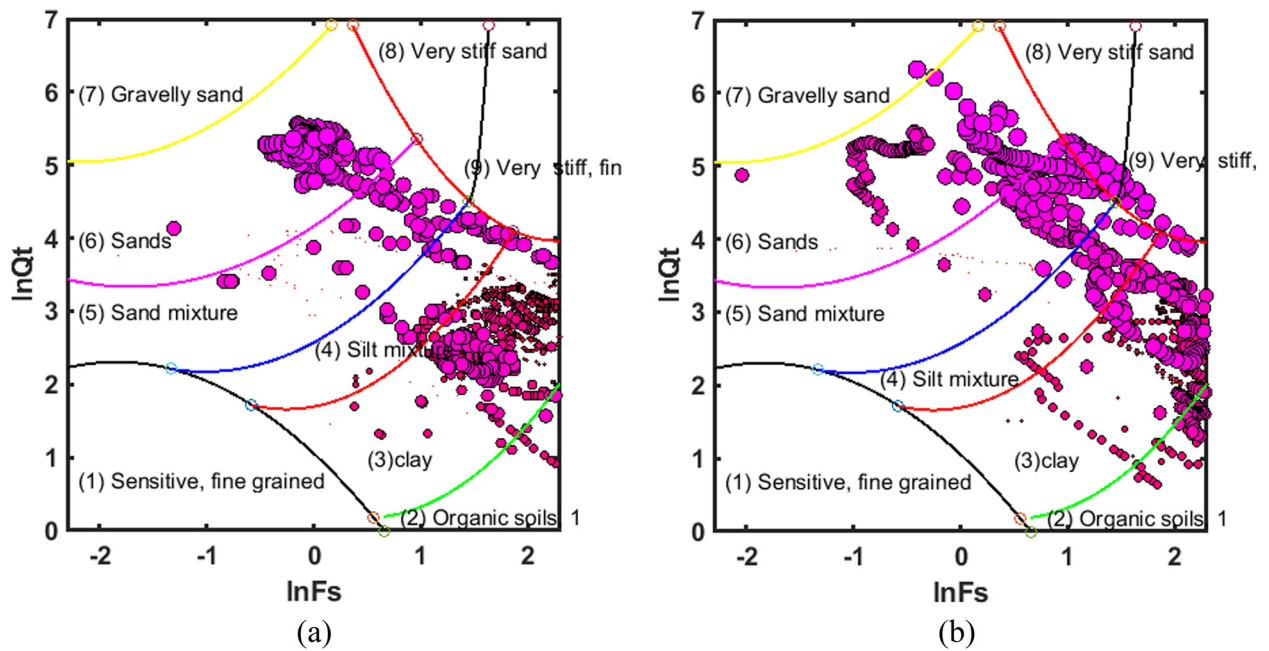


Figure 4: Points of $\ln Q_t$ and $\ln F_s$ in the physical space proposed by Robertson, 2010: (a) CPT3 and (b) CPT4.

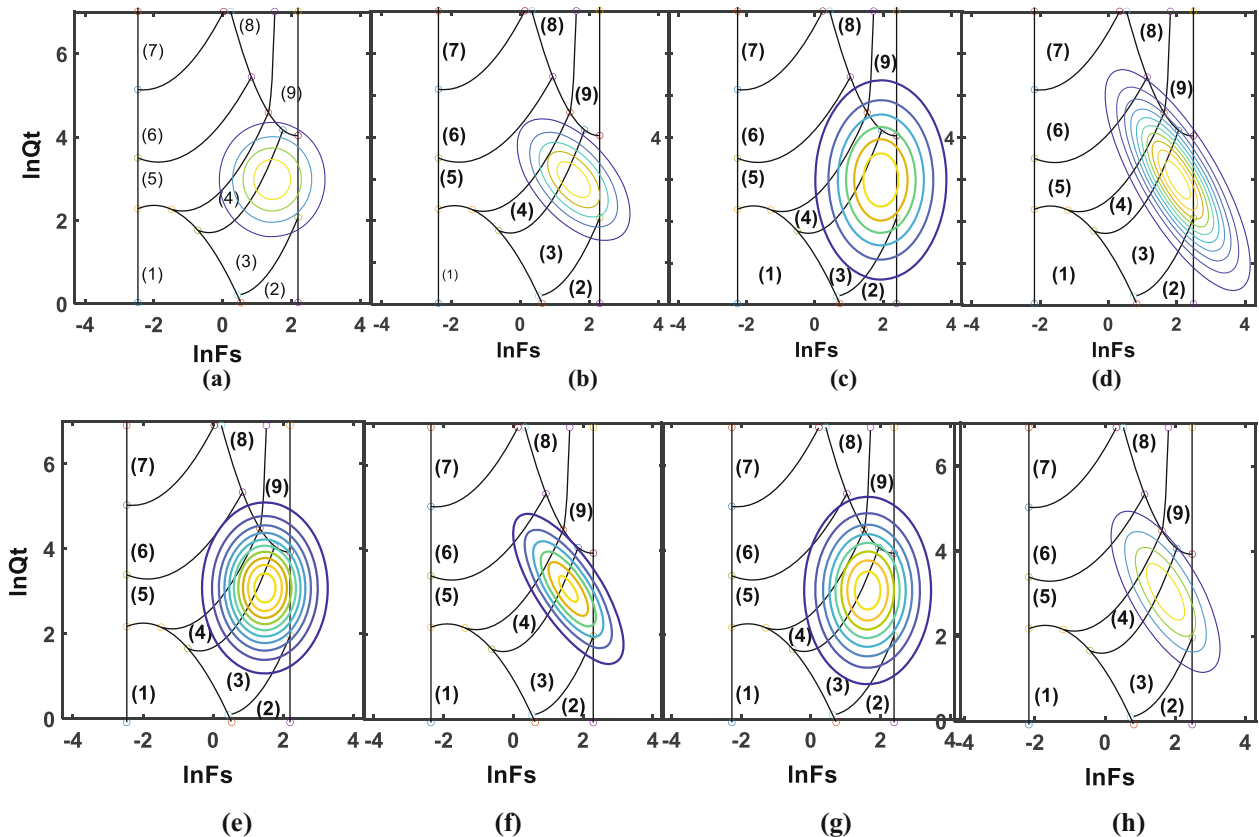


Figure 5: (a) Data of CPT1 on the Robertson chart simulated by DC matrix, (b) full matrix, (c) data of CPT2 on Robertson chart by DC, (d) full matrix, (e) data of CPT3 on Robertson chart by diagonal matrix, (f) full matrix, (g) data of CPT4 on Robertson chart by diagonal matrix, and (h) full matrix.

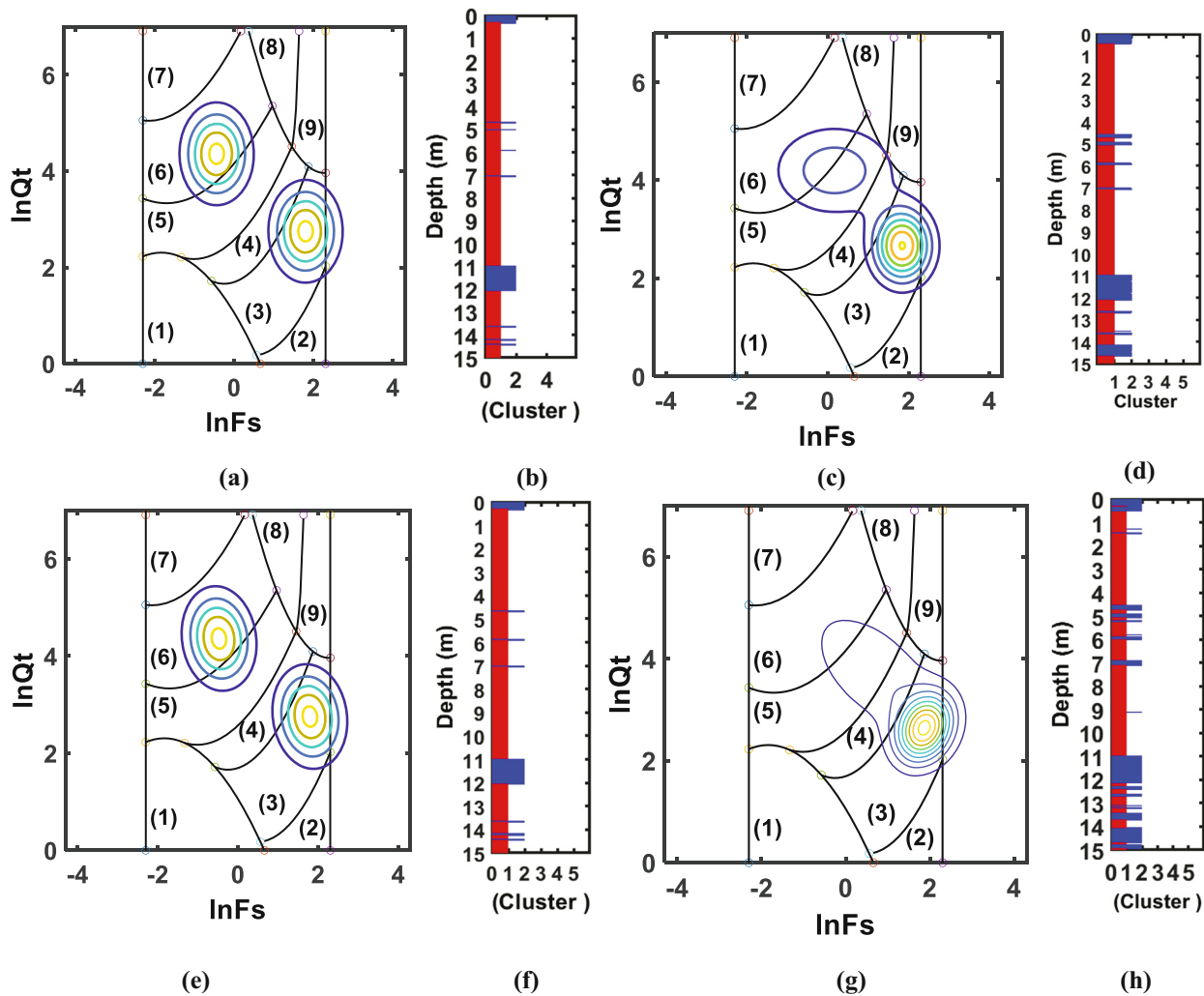


Figure 6: Feature and physical patterns of the CPT1 using four types of covariance: (a) feature spatial of CPT1, true DC, two clusters; (b) physical spatial of CPT1; (c) feature spatial of CPT1, false DC, two clusters; (d) physical spatial of CPT1; (e) Feature spatial of CPT1, true full covariance, two clusters; (f) physical spatial of CPT1; (g) feature spatial of CPT1, false full covariance, two clusters; and (h) physical spatial of CPT1.

[0.9275, -0.8845; -0.8845, 1.4331]. The covariance is negative, which means the $\ln Q_t$ decreases with an increase in the $\ln F_t$. Since the components of GMM are assumed to be single, the shared or non-shared covariance does not affect the result.

Figure 5e shows the distribution of points of CPT3 on the chart of Robertson. The center of the measured points represented by the ellipse that appeared on the Robertson chart occupies region number 3, representing the clay and silty clay. The correlation was negative since the top of the ellipse is oriented to the left of the vertical axis. Figure 7g shows the distribution of points of CPT3 on the chart of Robertson. The mean value of the component of the GMM = [1.5922, 3.1258] and the full covariance was [0.6597, -0.5480; -0.5480, 0.8345]. It is clear that the center of the points was in region number 3, which represents the clay, and the correlation was negative

since the rotation of the ellipse is about 150 from the x -axis clockwise.

Figure 5g shows the distribution of points of CPT4 on the Robertson chart. It is clear that the center of the points was in region number 3, which represents the clay, and the correlation was negative because of the rotation of the ellipse. Figure 5h shows the distribution of points of CPT4 on the Robertson chart. The center of the points was in region number 3, which represents clay and silty clay, and the correlation was negative since the rotation of the ellipse is greater than 90° from the x -axis clockwise. Generally, the DC that is used to represent the data of CPT4 shows a vertical distribution of the data more than the horizontal. The points typically extend vertically. For the second case, when the full covariance is used, the parameters correlate negatively.

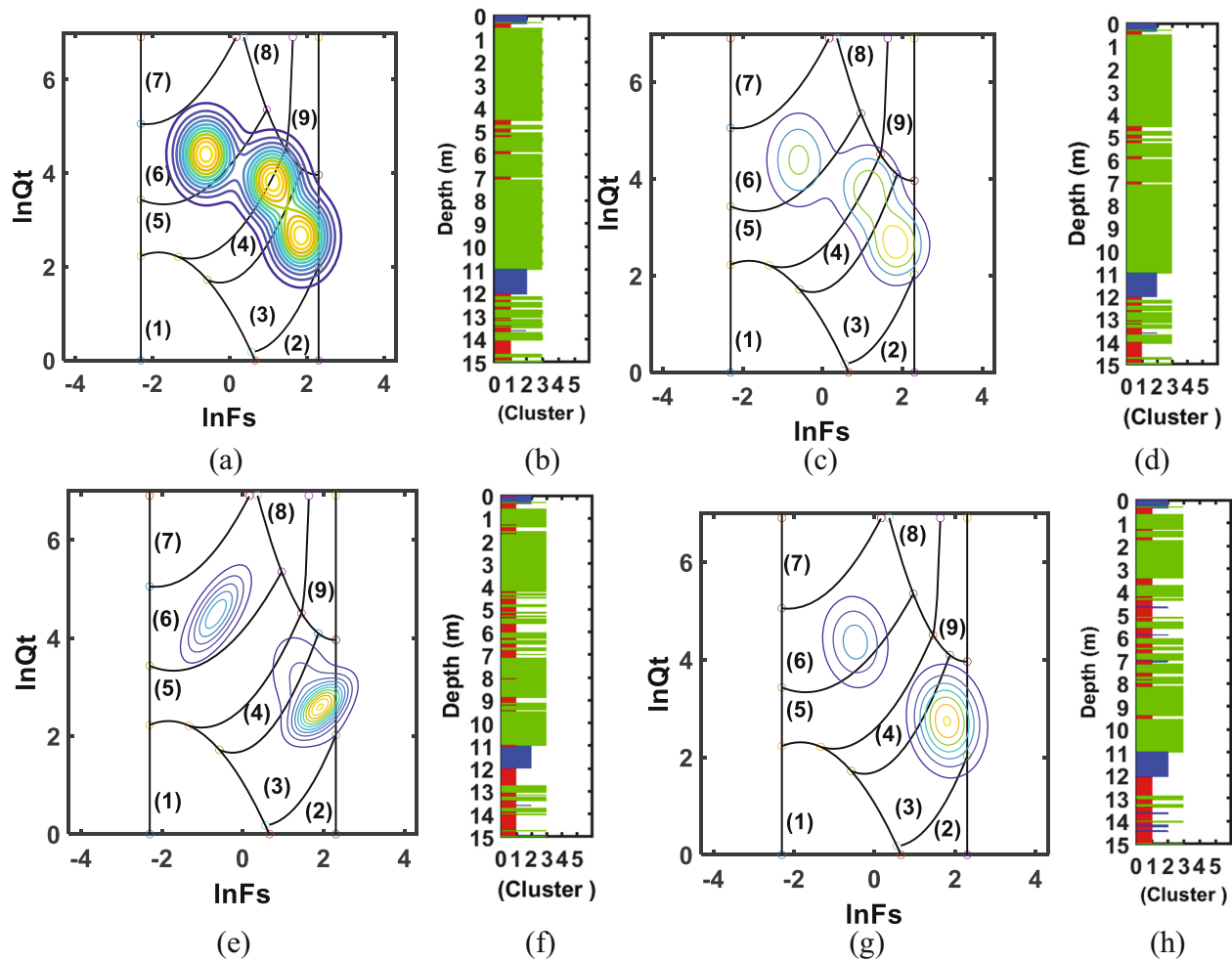


Figure 7: Three cluster model, in three model forms, for four cases of covariance: (a) Robertson chart, true DC, three clusters; (b) physical patterns; (c) Robertson chart, false full covariance, three clusters; (d) physical patterns; (e) Robertson chart, false DC, three clusters; (f) physical patterns; (g) Robertson chart, unshared full covariance, three clusters; and (h) physical patterns.

From the above results, the CPTs tested on the site showed clay and silty clay soil type and the single cluster extends on the Robertson chart along the boundaries of soil forms a negative correlation.

4.3 Two clusters with DC

Generally, according to the geological formation of the region, the soils in Nasiriyah are flood-plain sedimentary soil that is clay, silt, and sand or a mixture of these components. According to several boreholes adjacent to the CPTs, the soils were clay and silt, which form a high percentage of soil, while the sand represents the second level in the classification. According to that, as a case study, the research considered the two component models of GMM to explain the soil types. The two clusters distributed over the feature patterns covered two zones clay, silt, and sand

soil. The mean values for the two GMMs were $\mu_1 = [-0.2936, 4.3479]$ and $\mu_2 = [1.6123, 3.0722]$. The first mean value refers to clean sand, silty sand which represents zone 6, and the second cluster denotes the clay zone to silty clay (zone 3). For non-shared diagonal the correlation between the two variables was a positive correlation which means that the $\ln F_s$ increases as $\ln Q_t$ increases. In the case of two clusters with full covariance, the GMM simulates the CPT with two components. The model was fitted by suggesting a full covariance matrix. It is presented in Figure 6g. Using DC may be recommended at the first stage of the solution, and if it provides an inadequate results, full covariance can be used.

Figure 6g shows the ellipse that bounds the Robertson chart's distributed points. The mean of the first ellipse is $[0.7064, 3.7321]$ which is located in region 3 and the covariance shows a positive correlation $[1.8687 \ 2.6267; 1.2400 \ -0.5511]$, while the second ellipse extends along regions 4

and 5 at mean value $[-0.5511, 0.7890]$ with positive correlation $[0.1921, 0.0434; 0.0434, 0.1861]$.

The distribution with depth indicated that soil was sandy soil at a range of depth 11–12 and 14–15 m. This results agree with the actual distribution of soil with depth.

It is found that the data points are distributed in zone 3 and zone 5 when the diagonal and full covariance is used with the unshared type (Figure 6c and g). The two zones represent clay and silty clay soil and silty sand to sandy silt. However, the points on every zone do not need to form the equivalent focusing as deduced by the profile of clusters (physical spatial) with depth (Figure 7b and d) which refers to that one cluster taking the most sketch compared to other. This conclusion is compatible with the two different types of covariance (Figure 6a and e), but the soil was in zone 3 and 6. It is evident from the feature patterns of the Robertson chart represented by zones between boundary curves that may have more than one segment in one cluster, but they represent soil at different depths. Figure 7e shows that the first cluster on the Robertson chart distributes on more than one layer, such as the soil between a depth of 11 and 12 m and the soil at the top. This observation confirms the results reported in [24,25]. Similarly, it was worth noting that the one statistical cluster does not necessarily represent the same soil type. It may belong to more than one zone. The segments in one cluster are statistically the same as each other, but they may belong to more than one soil type, and they may have more than one soil behavior because they are distributed in more than one zone in the Robertson chart. Robertson and Cabal [5] constructed the classification chart by directly linking the feature pattern and soil mechanical behavior, represented by the cone tip resistance and sleeve friction measured by CPT. This may form the vital difference between the statistical and mechanical descriptions of the components measured.

5 Three GMM

This section presents the results of using the three cluster models for the measured data during CPT1 based on four types of covariance matrices. We can identify the center of Gaussian distribution for every layer in CPT. Assume no correlation exists between the probability decay directions for all Gaussian distributions, which results in a DC matrix. Figure 7 shows the distribution of the clusters on the Robertson chart using the four types of covariance matrices. In most cases, the data are not grouped as

circles as in the case of using the *k*-means technique [26], and it takes a different shape. In contrast, GMM appears as one-direction extended clusters. Further, the GMM becomes complex as the number of *k* increases.

The DC makes the major and minor axes of the ellipse parallel or perpendicular to the *x* and *y* axes (Figure 7a and b). The shared covariance indicated that all the components of GMM have the same covariance matrix. This is why all ellipses have the same size and orientation. Using full covariance (Figure 7e–h) allows for correlated predictors with no restriction for the size and orientation of the ellipse relative to the axis *y* and *x*. It can cause overfitting and may capture the correlation structure among the predictors. The ellipse center representing the Robertson chart's data is distributed in zones 3, 4, and 6. The concentration of data points in zone number 3 on the Robertson chart means that most of the depths of soil are clay and silty clay (Table 1).

6 Conclusion

Analysis of soil classification based on CPT measurement at four locations in Nasiriyah using GMM clusters utilizing four types of covariance matrices reveals some conclusions. The proposed method is sensitive to detecting the thin layers. Therefore, a soil profile with more details can be obtained, giving a chance to understand and interpret the CPT measurements. The thickness of the thin layers and the location of boundaries depend on the type of covariance matrix. The non-shared full covariance matrix reflects more layer boundaries and thin layers than the shared covariance matrix and DC matrix. It has also been found that the soil profile can be developed very fast since the layer boundaries indicated by the belonging of every soil unit to the corresponding clusters and no rich computational process were required like the Bayesian approach. It is concluded that the proposed method did not require an experience-based decision to classify the soil and indicate the layer boundaries. Further, the results are visually expressed and more practical and familiar for geotechnical engineers. However, this method may show some restrictions and limitations. It was found that the layer boundaries developed by the proposed method do not necessarily mean the existence of different soil types since they may be located in the same zone on the Robertson chart. Moreover, detecting the layer boundaries may refer to more than one type of soil. Hence, the probability of returning every point to a cluster is the required method that can be depended on.

Acknowledgments: The authors are grateful to the College of the Engineering/University of Thi-Qar for the general support and to the Engineering Consultant Bureau (ECB).

Funding information: The authors state no funding involved.

Author contributions: All authors have accepted responsibility for the entire content of this manuscript and approved its submission.

Conflict of interest: Authors state no conflict of interest.

References

- [1] Karkush MO, Ahmed MD, Sheikha AA, Al-Rumaithi A. Thematic maps for the variation of bearing capacity of soil using SPTs and MATLAB. *Geosciences*. 2020 Sep;10(9):329.
- [2] Karkush MO, Sabaa MR, Salman AD, Al-Rumaithi A. Prediction of bearing capacity of driven piles for Basrah governorate using SPT and MATLAB. *J Mech Behav Mater*. 2022 Jan 1;31(1):39–51.
- [3] Adel R, Shakir RR. Evaluation of the bearing capacity of a single pile by numerical analysis and various methods. *Yantu Gongcheng Xuebao/Chinese J Geotech Eng*. 2021;43(10):34–44.
- [4] Shakir RR. Probabilistic-based analysis of a shallow square footing using Monte Carlo simulation. *Eng Sci Technol Int J*. 2019;22(1):313–33.
- [5] Robertson PK. Soil classification using the cone penetration test. *Can Geotech J*. 1990;27(1):151–8.
- [6] Robertson PK. Cone penetration test (CPT)-based soil behaviour type (SBT) classification system – an update. *Can Geotech J*. 2016;53(12):1910–27.
- [7] Phoon K-K, Kulhawy FH. Characterization of geotechnical variability. *Can Geotech J*. 1999;36:612–24.
- [8] Jung BC, Gardoni P, Biscontin G. Probabilistic soil classification based on cone penetration tests. In: Kanda J, Takada T, Furuta H, editors. *Applications of Statistics and Probability in Civil Engineering: Proceedings of the 10th International Conference*; 2007 31 Jul – 3 Aug; Tokyo, Japan. CRC Press; 2007.
- [9] Campanella RG, Robertson PK, Gillespie D, Greig J. Recent developments in situ testing of soils. In: *Proceedings of 11th International Conference on Soil Mechanics and Foundation Engineering*; 1985 Aug 12–16; San Francisco (CA), USA. ISSMGE; 1985. p. 849–54.
- [10] Douglas BJ, Olsen RS. Soil classification using electric cone penetrometer. *Proceedings of Conference on Cone Penetration Testing and Experience*; 1981 Oct 26–30; St. Louis (MO), USA. p. 209–27.
- [11] Zhang Z, Tumay MT. Statistical to fuzzy approach toward cpt soil classification. *J Geotech Geoenviron Eng*. 1999;125(3):179–86.
- [12] Ching J, Wang JS, Juang CH, Ku CS. Cone penetration test (CPT)-based stratigraphic profiling using the Wavelet transform modulus maxima method. *Can Geotech J*. 2015;52(12):1993–2007.
- [13] Krogstad A, Depina I, Omre H. Cone penetration data classification by Bayesian inversion with a Hidden Markov model. *J Phys: Conf Ser*. 2018;1104:012015.
- [14] Wang Y, Cao Z. CPT-based probabilistic site characterization in geotechnical engineering. In: Deodatis G, Ellingwood BR, Frangopol DM, editors. *Safety, reliability, risk and life-cycle performance of structures and infrastructures. Proceedings of the 11th International Conference on Structural Safety and Reliability*; 2013 Jun 16–20; New York (NY), USA. CRC Press; 2014.
- [15] Huang K, Cao Z, Wang Y. CPT-based Bayesian identification of underground soil stratigraphy. In: Zhang L, Wang Y, Wang G, Dianqing L, editors. *Geotechnical Safety and Risk IV: Proceedings of the 4th International Symposium on Geotechnical Safety and Risk*; 2013 Dec 4–6; Hong Kong. CRC Press; 2013.
- [16] Cao ZJ, Zheng S, Li DQ, Phoon KK. Bayesian identification of soil stratigraphy based on soil behaviour type index. *Can Geotech J*. 2019;56(4):570–86.
- [17] Wang X. Uncertainty quantification and reduction in the characterization of subsurface stratigraphy using limited geotechnical investigation data. *Undergr Space (China)*. 2020;5(2):125–43.
- [18] Wang X, Wang H, Liang RY, Zhu H, Di H. A hidden Markov random field model based approach for probabilistic site characterization using multiple cone penetration test data. *Struct Saf*. 2018;70:128–138.
- [19] Farhadi MS. An Integrated Optimization-Game Theory Model for CPT-based Subground Stratification. 29th European Safety and Reliability Conference; 2019 Sep 22–26; Hannover, Germany.
- [20] Tsuda Y, Kagehira M. Stratigraphic profiling using sparse modeling. 29th European Safety and Reliability Conference; 2019 Sep 22–26; Hannover, Germany.
- [21] Shakir RR. Selecting the probability distribution of cone tip resistance using moment ratio diagram for soil in Nasiriyah. *Geotech Geol Eng*. 2019;37:1703–28.
- [22] Shakir RR. Spatial correlation of cone tip resistance for soil in Nasiriyah. *Open Civ Eng J*. 2018;12:413–29429.
- [23] Ali HM, Shakir RR. Geotechnical map of Thi Qar governorate using geographical information systems (GIS). *Mater Today Proc*. 2022;60(Part 3):1286–96.
- [24] Wang H, Wang X, Wellmann JF, Liang RY. A Bayesian unsupervised learning approach for identifying soil stratification using cone penetration data. *Can Geotech J*. 2019;56(8):1184–205.
- [25] Wang H. Finding patterns in subsurface using Bayesian machine learning approach. *Undergr Space*. 2020;5(1):84–92.
- [26] Shakir RR, Jawad T, Mohammad A-U. Soil profile stratification based on cone penetration test results using k-means and hierarchical clustering. 3rd Conference of the Arabian Journal Geoscience (CAJG); 2020 Nov 2–5; Sousse, Tunisia.